

THE SHORT CIRCUMFERENCE DAMPING RING DESIGN FOR THE ILC

M. Korostelev, F. Zimmermann, CERN, Geneva, Switzerland;
K. Kubo, M. Kuriki, S. Kuroda, T. Naito, J. Urakawa, KEK, Ibaraki, Japan;
M. Ross, SLAC, Menlo Park, California, USA

Abstract

The ILC damping ring tentative design is driven by the operational scenario of the main linac, the beam-dynamics demand of producing a stable and high-quality beam, the injection/extraction scheme and the kicker performance. In this paper, a short circumference damping ring design based on TME cells is described. The ring accommodates injection kickers which provide a flat top of 280 nsec and a 60 nsec rise and fall time and very fast strip-line kickers for beam extraction with a 2 nsec rise and fall time for 3-MHz operation.

INTRODUCTION

The original TESLA design featured a 17-km long “dog-bone” damping ring [1]. Due to the large circumference, this damping ring must operate with local long-distance “coupling bumps” in order to achieve an acceptable space-charge tune shift, and it can be sensitive to various types of instabilities and perturbations, such as linac stray fields or ground motion. An advantage of the large circumference are the loose kicker requirements. However, despite of this large circumference the bunches still need to be extracted individually from the damping ring, since the bunch spacing in the 17-km ring of about 20 ns is much shorter than the 3-ns spacing in the superconducting linac.

Ongoing worldwide studies, e.g., in [2], suggest that it may be possible to build kicker magnets with significantly shorter rise and fall times, of the order of a few ns. Given this possibility of faster kickers for injection and extraction, a ring with a smaller circumference then becomes an attractive option. We here report about one such design, which has a circumference of 3 km.

DESIGN STRATEGY

The starting point of the damping-ring optimization was the KEK design “TME5.1” of a 3-km ILC damping ring, created by S. Kuroda [3]. This ring design combined TME-cell arcs adopted from the NLC damping ring design with 80 ATF-type wigglers at the center of each arc, and long empty straight sections. The wigglers covered two times a total length of 160 m and had the ATF wiggler period of 40 cm. The length of the arc bending magnet was 9 m. The ring energy of 5 GeV was chosen as in the TESLA design [6].

The emittance performance of this ring was recently improved by modifying both the wiggler parameters and the arcs. The optimization was based on the expression for the equilibrium emittance without intrabeam scattering for a

hard-edged wiggler model [4],

$$\gamma\epsilon_x = \frac{C_q\gamma^3}{12(J_{x0} + F_w)} \left[\frac{\epsilon_r\theta^3}{\sqrt{15}} + \frac{F_w|B_w^3|\lambda_w^2 \langle \beta_x \rangle_w}{16(B\rho)^3} \right], \quad (1)$$

where

$$F_w \approx \frac{L_w B_w^2}{4\pi(B\rho)B_a} \quad (2)$$

and $\theta = B_a L_a / (B\rho)$.

First, the wiggler period λ_w was reduced from 40 cm to 27 mm, which is the period of the NLC wiggler design [5]. As a next step, using Eq. (1), $\gamma\epsilon_x$ was computed as a function of the arc and wiggler fields B_a and B_w . The arc bending field was next decreased from 1.94 kG to 1.535 kG, and at the same time the total number of arc cells increased from 69 to 76, thereby reducing θ in (1). Equation (1) suggests that decreasing B_w would further reduce the emittance. However, this is not the case at the design bunch population of 2×10^{10} , if intrabeam scattering is taken into account (see Fig. 4 below). Therefore, the wiggler field was left at 21.5 kG. The length of a wiggler consisting of 8 periods is about 2 m, matching the FODO cell length in the straight sections. The optics between wiggler sections and arcs was rematched.

The rf frequency was left at the original value of 714 MHz (the same frequency as in the SLC damping rings or the ATF), as increasing the frequency by a factor of 2 aggravates the effect of intrabeam scattering. Different beam energies were not studied.

In Table 1 the original parameters for the “TME5.1” design are compared with those obtained after modifying the wigglers or both the wigglers and the arcs, respectively. Figure 1 shows the horizontal beta function around the ring, which gives an impression of the overall layout.

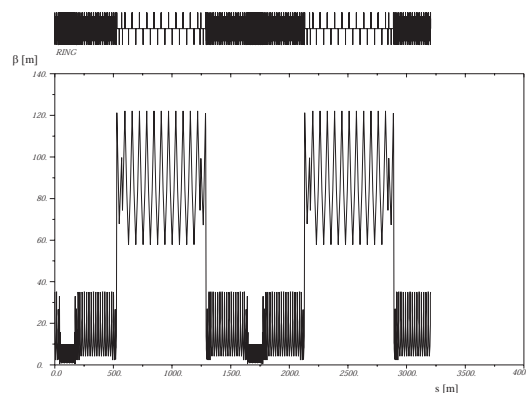


Figure 1: Horizontal beta function around the 3-km damping ring.

Table 1: Parameters of three ILC damping-ring designs with 3-km circumference

Parameter	TME5.1	with NLC wiggler	with NLC wiggler and modified arcs
Ring energy [GeV]	5.0	5.0	5.0
Ring circumference [m]	3223.8	3223.8	3201.0
No. of bunch trains stored	60	60	31
No. of bunches/trains stored	43	43	100
Train spacing [ns]	61	61	67
Bunch spacing [ns]	2.8	2.8	2.8
Bunch population	1.4×10^{10}	1.4×10^{10}	2.0×10^{10}
Horizontal emittance (norm) [nm]	3892	2841	2030(2200)
rms energy spread [%]	0.136	0.15	0.151
rms bunch length [mm]	7.37	9.94	9.6
Damping time x/y/z [msec]	12.1/12.1/6.08	8.1/8.1/4.05	8.12/8.12/4.6
Betatron tune x/y	45.36/24.55	45.36/24.78	48.85/27.19
Number of cells	60	60	76
Field of bending magnet [T]	0.194	0.194	0.153
Length of bending magnet [m]	9	9	9
Number of wigglers	80	80	80
Wiggler period [cm]	40	27	27
Field of wiggler [T]	1.8	2.15	2.15
Energy loss per turn [MeV]	8.85	13.28	13.15
RF frequency [MHz]	714	714	714
Effective RF voltage [MV]	16	16	16
Momentum compaction	3.6×10^{-4}	3.6×10^{-4}	3.5×10^{-4}

PERFORMANCE

The performance evaluation takes into account the effect of radiation damping, quantum excitation, and intrabeam scattering, as described for the CLIC damping ring design in [7, 8]. The intrabeam scattering contribution is computed using the “modified Piwinski formalism” [9, 10]. Figures 2 and 3 present the emittance evolution after injection, assuming injected beam emittances of $\gamma\epsilon_x \approx 120 \mu\text{m}$ and $\gamma\epsilon_y \approx 60 \mu\text{m}$. The contribution from intrabeam scattering is not negligible. Nevertheless, this ring achieves a final horizontal emittance of $2 \mu\text{m}$, which is a factor four below the ILC target value and factor two improvement compared with “TME5.1”.

Figure 4 compares the horizontal equilibrium emittances for wiggler fields of 21.5 kG and 15.6 kG. At bunch populations above $N_b \approx 1.7 \times 10^{10}$, the higher wiggler field yields a smaller emittance. For the stronger field, the equilibrium bunch length is about 50% higher, independent of the bunch population, as is illustrated in Fig. 5.

Figure 6 displays the on-momentum dynamic aperture obtained by tracking. The horizontal and vertical amplitudes on the two axes are expressed in terms of the final rms beam sizes. The maximum beam emittances which could be injected into the dynamic aperture of this ring are about $\gamma\epsilon_x \approx 1000 \mu\text{m}$ and $\gamma\epsilon_y \approx 60 \mu\text{m}$. Figure 7 illustrates the nonlinear chromaticity.

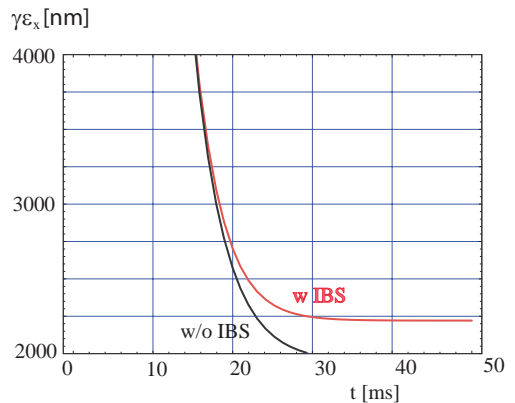


Figure 2: Normalized horizontal emittance as a function of time computed with and without intrabeam scattering.

Intrabeam scattering was included in all emittance calculations presented here. The importance of other collective effects can be estimated as for CLIC in Ref. [11].

CONCLUSION

The 3-km damping ring presented here provides an emittance of $\gamma\epsilon_x \approx 2 \mu\text{m}$, i.e., 4 times smaller than the ILC target, and it has a circumference of about 3 km. The horizontal dynamic aperture is sufficiently large to accept a beam

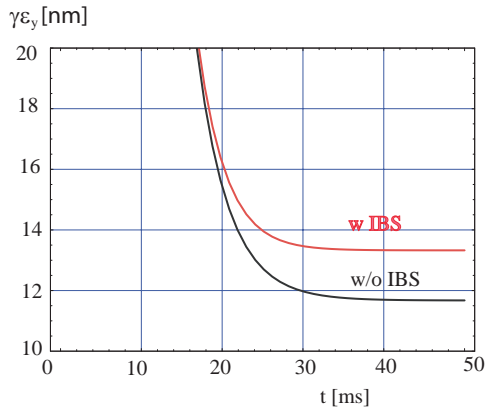


Figure 3: Normalized vertical emittance as a function of time computed with and without intrabeam scattering; and assuming 0.6% betatron coupling.

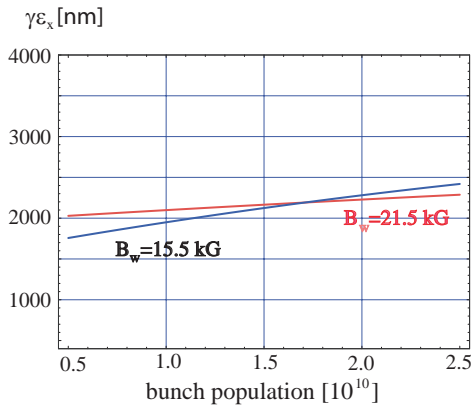


Figure 4: Horizontal equilibrium emittance as a function of bunch population with intrabeam scattering for two different values of the wiggler field, assuming 0.6% betatron coupling.

of $\gamma\epsilon_{x0} \approx 0.01\text{m}$. The vertical acceptance corresponds to about $60 \mu\text{m}$. Further optimization is possible.

REFERENCES

- [1] W. Decking, "Optical Layout for the TESLA 5-GeV Damping Ring," DESY-TESLA-2001-11 (2001).
- [2] L. Emery et al., "Studies Pertaining to a Small Damping Ring for the International Linear Collider," FERMILAB-TM-2272-AD-TD (2004).
- [3] J. Urakawa, "Alternative DR Designs – Overview," First ILC KEK Meeting, November 14, 2004.
- [4] P. Emma, T. Raubenheimer, "Systematic Approach to Damping Ring Design," PRST-AB 4, 021001 (2001).
- [5] J. Corlett et al., "NLC Damping Ring Wiggler Studies 1999," LCC-0031 (1999); J. Corlett, S. Marks, M.C. Ross, "Transverse Field Profile of the NLC Damping Rings Electronmagnet Wiggler," LCC-0038, CBP Tech-Note-234 (2000).
- [6] W. Decking, R. Brinkmann, EPAC 2000 Vienna (2000).
- [7] M. Korostelev, F. Zimmermann, "Optimization of CLIC Damping Ring Design Parameters," EPAC'02 Paris (2002).

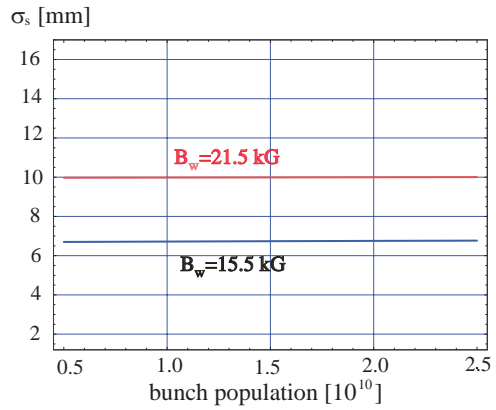


Figure 5: Equilibrium rms bunch length as a function of bunch population with intrabeam scattering for two different values of the wiggler field, assuming 0.6% betatron coupling.

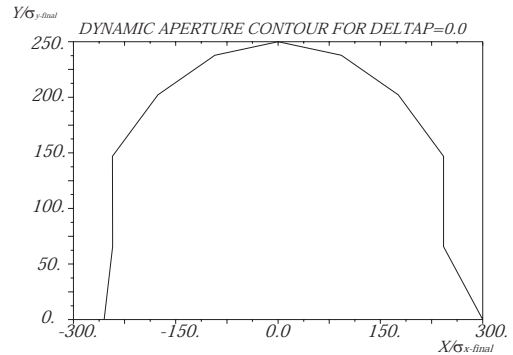


Figure 6: Dynamic aperture in units of the final beam sizes.

- [8] M. Korostelev, F. Zimmermann, Proc. Nanobeam'02 Lausanne, CERN-Proceedings-2003-001 (2001).
- [9] A. Piwinski, 9th HEACC'74 Stanford (1974).
- [10] K.L.F. Bane, EPAC'02 Paris (2002).
- [11] F. Zimmermann et al., "Collective Effects in the CLIC Damping Rings," these proceedings.

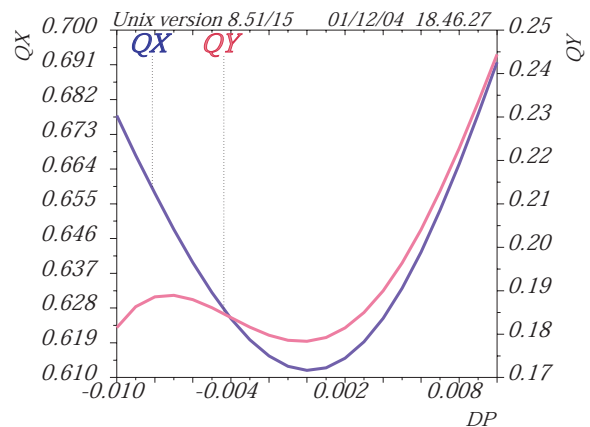


Figure 7: Nonlinear chromaticity.